RSC Advances

ROYAL SOCIETY OF CHEMISTRY

www.rsc.org/advances

Cite this: DOI: 10.1039/c0xx00000x

www.rsc.org/xxxxxx

ARTICLE TYPE

Synthesis of 5, 10, 15, 20-tetrakis (4-naphtalen-2-yl-benzoate) porphyrin, its complexes with Zinc and Cobalt and Fe_3O_4@ZrO_2-TNBP as photocatalyst and investigating its photocatalytic activities

Hossein Ghafuri*[a], Zahra Movahedinia[a], Rahmatollah Rahimi[a] and Hamid Reza Esmaili Zand[a]

Received (in XXX, XXX) XthXXXXXXXXX 20XX, Accepted Xth XXXXXXXXX 20XX
DOI: 10.1039/b000000x

Abstract: 5,10,15,20-tetrakis(4-naphtalen-2-yl-benzoate) porphyrin and its porphyrin complexes with zinc and cobalt and Fe_3O_4@ZrO_2 -TNBP photocatalyst were synthesized with high yields and the structure and morphology were characterized by X-ray diffraction (XRD), UV–Vis, FT-IR and ^1H-NMR spectroscopy and scanning electron microscopy (SEM). The photocatalytic activity was investigated by photo degradation of methylene blue in aqueous solution under visible light irradiation. The results demonstrated that porphyrin significantly enhanced the visible photocatalytic activity of Fe_3O_4@ZrO_2 magnetic nanoparticles in the degradation of methylene blue. Also these findings demonstrate that Fe_3O_4@ZrO_2 -TNBP photocatalysts exhibited higher photoactivity than bare Fe_3O_4@ZrO_2 nanoparticles under light irradiation.

Introduction

A 4n+2 aromatic macrocycle of porphyrin including pyrroles and methine carbons in square plane is one of the most major pigments that could be found in nature. Because of enormous properties of porphyrin like its coordination chemistry, emission capabilities, optical and electronic abilities, a range of porphyrins and conjugated porphyrin arrays have been composed along the years[1-4]. Porphyrins and its derivatives are predominantly considerable pieces in reactions and have several properties. Catenanes and rotaxanes that owing porphyrins, resulted in new categories with different properties. They incorporating the electronic properties of porphyrins in their states with linked compounds. Photosynthesis in certain bacteria and plants is mainly founded on porphyrinoid pigments. Porphyrinic macrocycles are modulated into arrays in the Polymerase Chain Reaction (PCR~~s~~), where light energy is finally converted to chemical energy. Also tris and tetrakis-porphyrin arrays are played their roles in PCR~~s~~[5]. Porphyrins play the key roles in a numerous synthetic multicomponent reactions at simulating the operation of the photosynthetic reaction centres[6]. Also, as the light resulting component of dye-sensitised nanocrystalline TiO_2 solar cells, porphyrins present enormous potential in this process[7].

Porphyrins have well absorptions and can be used for reduce pollutants of phenols (with photo oxidation of them). Tetrakis porphyrin and its metal derivatives also is a strong sensitizer for this action[8].

In the earth's history, Natural metalloporphyrins were formed early and performed a significant function in transport goals in biological activities; also in redox reactions, metabolism and photosynthesis. Metalloporphyrins are mostly appropriate for tailoring sensors and catalysts with functionalization the surface on the nanoscale[9].

After seeing the abilities of porphyrins and metalloporphyrines[10] and also the importance of purification of water that contaminated by waste water, the properties of metalloporphyrins have been widely considered for purification of water.

Entering the organic contaminants in drinking water through industrial waste water containing dyes, due to increasing the uses of them causes serious problems. Biological purification of these pollutants due to the limited effectiveness is not appropriate. There are special attention to removal or degradation many contaminants, including methylene blue using metalloporphyrins absorbents.

On the other hand, magnetic nanoparticles because of their high capacity load transfer and easy separation by an external magnetic field has attracted the attention of many researchers. Nanoparticles have wide applications in data storage, sensors, catalysts, biotechnology and environmental fields. Superparamagnetic Fe_3O_4 nanoparticles due to high levels of chemical and magnetic dipole interactions are very sensitive to oxidation and aggregation. Different methods are used to protect and prevent their oxidation. Among them using of metal oxides such as ZrO_2 and magnetic nanoparticles Fe_3O_4@ZrO_2 can be useful superseded for organic and inorganic substrates to established porphyrins[10-12].

Our researches shows that the porphyrin with its four pyrrolic rings set on a square surrounding substance (and metalloporphyrin) improved the photocatalytic performance of Fe_3O_4@ZrO_2 magnetic nanoparticles on the degradation of organic pollutants. These findings demonstrate that Fe_3O_4@ZrO_2-

TNBP photocatalysts exhibits higher photoactivity than bare Fe_3O_4@ZrO_2 nanoparticles under light irradiation.

Due to these extensive uses of porphyrins, we also drew attention to this compound and we decided to synthesis the metalloporphyrin[13-14]. In 2014, Xiangqing Li and coworkers reported the synthesis of silanized porphyrin cobalt monomer[15] and we used their method to synthesize 5, 10, 15, 20-tetrakis (4-naphtalen-2-yl-benzoate) porphyrin and its metal complexes with zinc and cobalt. We synthesized Fe_3O_4@ZrO_2-TNBP as photocatalyst and used it as a substrate of Zn and Co porphyrin. Its photocatalytic efficiency on the degradation of methylene blue under visible light irradiation was examined and the results indicated that porphyrin can greatly enhance the visible photocatalytic activity of Fe_3O_4@ZrO_2 magnetic nanoparticles on the degradation of methylene blue. We found the electron transfer from porphyrin to Fe_3O_4@ZrO_2 magnetic nanoparticles plays a strategic role in the photocatalytic processes of the Fe_3O_4@ZrO_2-TNBP system and thus it leads to increase the photocatalytic activity.

Experimental

Materials and methods

All of the chemicals used in this work were obtained from Merck and used without further purification.

^{1}H-NMR spectra were recorded with a Bruker Avance 500 MHz, in chloroform with tetramethylsilane (Me_4Si) as an internal standard. Infrared (IR) spectra were carried out on a Shimadzu FT-IR-8400S spectrophotometer using a KBr pellet. The DRS spectra were prepared via a Shimadzu MPC-2200 spectrophotometer. The UV-Vis spectra were recorded on a Shimadzu (mini 1240 double beam) spectrophotometer in the wavelength range of 400-800 nm. The particle morphologies were observed by scanning electron microscopy (SEM) at 26 kV (KYKY- EM3200). The X-ray diffraction measurement was performed using graphite monochromatic copper radiation (Cu Kα) at 40 kV, 40 mA over the 2θ range of 5–80◦. Magnetic properties of the particle were assessed with a vibrating-sample magnetometer (VSM, Lake Shore 7410). A commercial HH-15 model vibrating sample magnetometer was utilized for the collection of magnetic particles.

Synthesis of 5,10,15,20 tetrakis (4-naphtalen-2-yl-benzoate) porphyrin

In the first step, TCPP (0.1 g, 0.1 mmol) was dissolved in THF (10 mL). Then thionyl chloride (1mL) was added drop wise to this solution, and after the addition was completed, the solution was stirred at 70°C for 2 h. After this the excess thionyl chloride was removed by rotary, and the remaining material was dissolved in THF (10 mL) and then β-Naphthol (0.06 g, 0.4 mmol) was added into this solution. The mixture was refluxed at 70°C for 8 h. Finally, TNBP was obtained after filtration. IR (KBr): ν_{max}= 3278, 2925, 2860, 1716, 1272, 808, 646 cm^{-1}. UV-Vis: λ_{max}= 420 nm (Soret band), 514,549, 589, 645 nm (Q bands).

Synthesis of Zn (II) 5,10,15,20 tetrakis (4-naphtalen-2-yl-benzoate) porphyrin (ZnTNBP)

Zn $(CH_3COO)_2$ (0.1 g, 6 mmol) and TNBP (0.15 g, 1 mmol) were dissolved in 50 mL DMF and refluxed for 3 h. After the solution was cooled at room temperature, the participated was collected by filtration, washed with water and dried in vacuum. IR (KBr): ν_{max}= 2923, 2854, 1716, 1272, 802, 713 cm^{-1}. UV-Vis: λ_{max}= 420 nm (Soret band), 513,547 nm (Q bands).^{1}*H*-NMR (500 MHz, $CHCl_3$): δ in ppm = 8.64-8.43 (s, 8H, CH pyrrol), 8.42-8.2 (m, 28 H, CH β-Naphthol), 8.02-8.1 (d, 8H, CH Ar), 7.72-7.64 (d, 8H, CH Ar).

Synthesis of Co (II) 5,10,15,20 tetrakis (4-naphtalen-2-yl-benzoate) porphyrin (CoTNBP)

For synthesis of CoTNBP, a mixture of $CoCl_2$ (0.09 g, 6 mmol) and TNBP (0.09 g, 1 mmol) was dissolved in 25 mL DMSO and the solution was refluxed at 190 °C for 24 h[16]. A brown precipitate was obtained, which was filtered and then purified by column chromatography and dried in vacuum. IR (KBr): ν_{max}= 2925, 2856, 1716, 1271, 811, 640 cm^{-1}. UV-Vis: λ_{max}= 428 nm (Soret band), 548 nm (Q band).

Preparation of Fe_3O_4@ZrO_2-TNBP photocatalyst

Fe_3O_4@ZrO_2-TNBP photocatalyst was obtained by mixing of TNBP (0.01 g) and Fe_3O_4@ZrO_2 nanoparticles (0.1 g). The mixture was dissolved in 50 mL DMF and the solution stirred and refluxed for 6 h. The solid product was collected by filtration, washed with water and dried in vacuum.

Photocatalytic degradation

For 30 mL of the MB aqueous solution ($C_\circ$ = 72 mol. L^{-1}), 30 mg of Fe_3O_4@ZrO_2-TNBP photocatalyst was used. Before irradiation, the suspension was stirred in the dark condition for 30 min. Then, in the presence of irradiation, samples were taken every 30 min in 4 h. The photocatalytic degradation of the samples was recorded by UV-Vis spectrum.

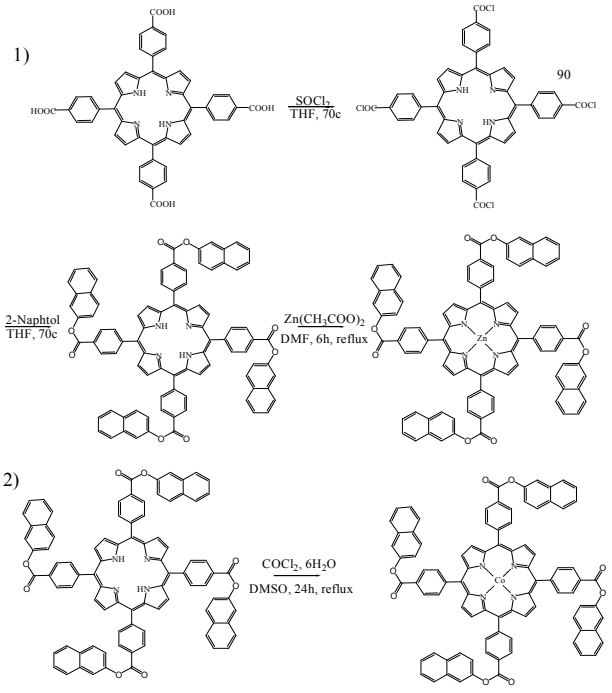

Scheme 1. Synthesis of 1) ZnTNBP, 2) CoTNBP

Result and discussion

According to scheme 1, tetrakis(4-naphtalen-2-yl-benzoate) porphyrin (TNBP) and its complexes with zinc and cobalt were synthesized and characterized by UV–Vis and FT-IR spectra.

FT-IR spectra analysis

The FT-IR spectra in KBr were recorded in the range of 400 - 4000 cm^{-1}. As shown in Fig. 1, the carbonyl vibration band C=O of a ester group appears as an intense band in 1716 cm^{-1} and indicates that the relative TNBPs were successfully synthesized. The N-H bending vibration band appears at 3200 cm^{-1} that approves pyrrole ring. C-H stretching of Ar group vibrations appears in 2900 cm^{-1}. Moreover disappearance of N-H in Fig. 2 vibration around 3200 cm^{-1} in this spectrum shows that the related metalloporphyrins were also quantitatively prepared.

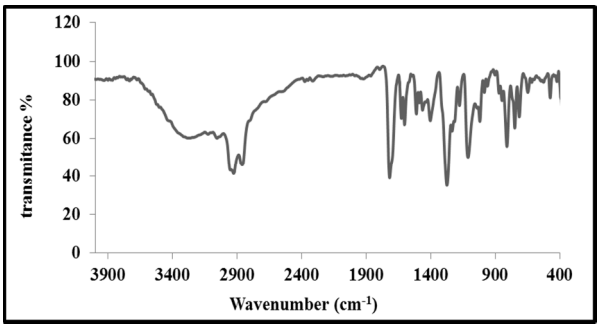

Fig 1. FT-IR spectrum of TNBP

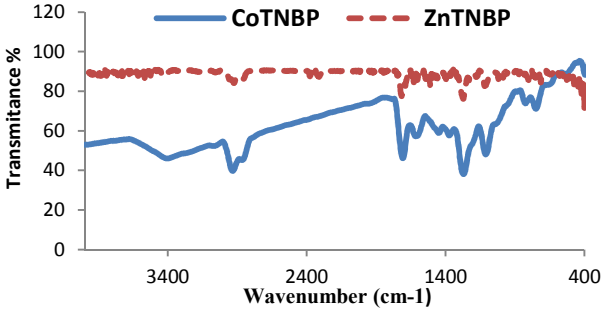

Fig 2. FT-IR spectra of metalloporphyrins

UV-Vis spectra analysis

UV-Vis absorption spectra of TNBP and its metal complexes in DMF in Fig. 3 indicate that the soret bands of TNBP and ZnTNBP appear in the region of 420 nm. Four weaker absorptions which relate to Q bands appear at higher wavelengths (about 500-650 nm). The coordination of TNBP with zinc and cobalt reduces the intensity of the soret band and the number of the Q bands from 4 bands to 2 bands, which apparently show that metalloporphyrins are produced and due to their symmetry, weak bands reduced. Because of d^{10} orbitals of Zn, it has very little effects on the Gap energy transfer of $\pi \rightarrow \pi^*$ in the porphyrin ligand. This makes soret and Q bands of porphyrin (TNBP and ZnTNBP) appear at around the same area.

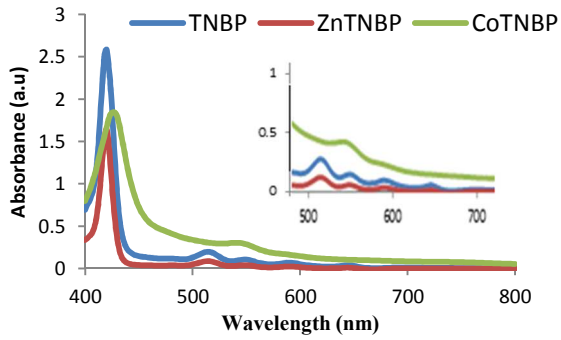

Fig 3. UV-Vis absorption spectra of TNBP and metalloporphyrin in DMF

DRS analysis

According to DRS spectra in Fig. 4, we find that there is no absorption above 400 nm for Fe_3O_4@ZrO_2, while the supported catalyst shows the characteristic peaks of soret band and Q bands and makes apparent that porphyrin successfully established onto the Fe_3O_4@ZrO_2 nanoparticles surface even as maintaining the porphyrin structure.

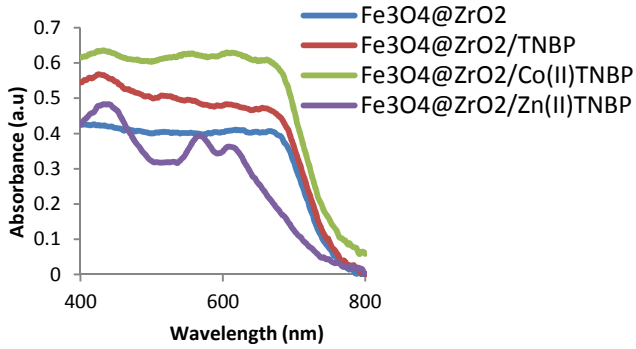

Fig 4. DRS spectra of Fe_3O_4@ZrO_2 /porphyrin

XRD study

The sensitized magnetic nanoparticles by ZnTNBP porphyrin, were analyzed by XRD (Fig. 5). Since porphyrins are amorphous and magnetic nanoparticls are crystalline, XRD pattern does not show the exact structure of the porphyrin. As can be seen, porphyrins reduces the intensity of nanoparticles peaks, but did not cause a change in the crystal structure of Fe_3O_4@ZrO_2 nanoparticles. Peaks appeared at 30.9 and 44.35 degrees are for Fe_3O_4 and peaks appeared on 21.28, 5.31, 17.34, 19.50 and 1.60 degrees are related to the structure of ZrO_2. According to this data, the structure of nanoparticle is monoclinic that is corresponding to the ZrO_2 standard card (01-083-0944) and Fe_3O_4 standard card (01-085-1436).

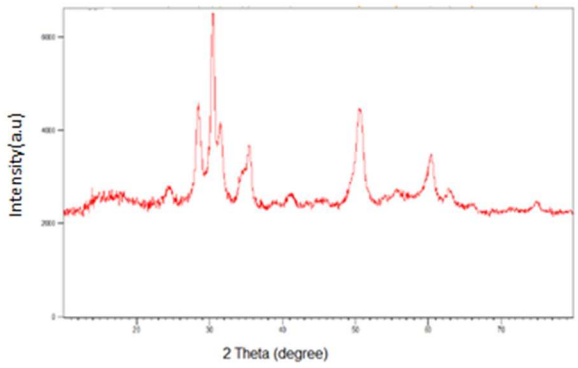

Fig 5. XRD pattern of Fe_3O_4@ZrO_2-ZnTNBP

SEM study

By SEM images, morphology, particle size and surface uniformity can be identified. SEM images of Fe_3O_4@ZrO_2 and Fe_3O_4@ZrO_2-ZnTNBP nanoparticles are shown in Fig. 6. Size of nanoparticles are between 37 to 61 nm. According to the pictures, nanoparticles are spherical and have a good uniformity. As can be seen, porphyrin is not created change in the monoclinic morphology of the nanoparticles.

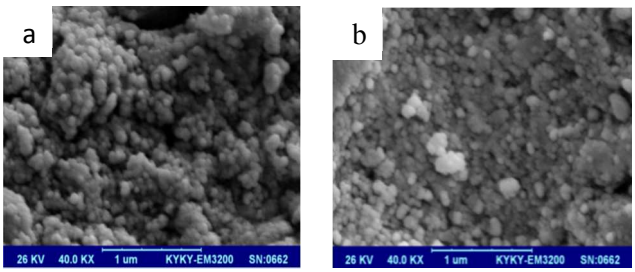

Fig 6. SEM images of nanoparticles of a) Fe_3O_4@ZrO_2 and b) Fe_3O_4@ZrO_2-ZnTNBP

VSM spectrum of Fe_3O_4@ZrO_2-ZnTNBP

In the results of the analysis of a vibrating sample magnetometer spectrum, which given in the Fig. 7, it is estimated that magnetic nanoparticles was reduced their super magnetic behavior after composition with porphyrin.

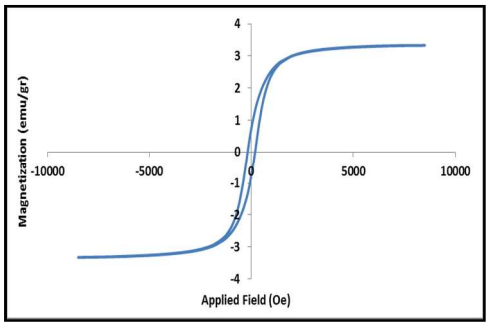

Fig 7. VSM Spectra of Fe_3O_4@ZrO_2-ZnTNBP

Investigation of the photodynamic degradation of methylene blue (MB)

To evaluate and compare the use of synthesized photocatalysts, degradation of methylene blue was done in concentration of 10 ppm in the presence of light (lamp LED 5W). Results after three hours of exposure by UV-Vis spectra were recorded on a chart. As can be seen in Fig. 8, porphyrins with different functional groups have different degradation on the substrate nanoparticles. Result of degradation ratio is given in the table 1.

Phenyl rings of TNBP were attached by π bond and van der Waals to the surface of the magnetic nanoparticles of zirconia iron oxide and in effect of ring resonance, electron transfer action has done better and results the increases of the degradation of methylene blue into nanoparticles. The greater the number of phenyl rings, resonance and electron transfer to destroy pollutants increased. But tetra (4-carboxyphenyl) porphyrin is better than TNBP to inclusion on the nanoparticle surface due to established hydrogen bonds by the carbonyl group and the hydroxyl group with surface area of the nanoparticles. As a result, electron transfer done easier and better, and the degradation of methylene blue to TNBP increased.

Metals in the center of tetra pyrrole rings of porphyrin increased more photocatalysis activity compared to the free porphyrin. Metalloporphyrins with the electron transfer (from the metal to the ligand) enhances catalyst activity and the degradation percentage of methylene blue.

Table 1. Result of degradation percentage

Catalyst	Degradation percentage
Not Catalyst	10
Fe_3O_4@ZrO_2	24
Fe_3O_4@ZrO_2/TNBP	57
Fe_3O_4@ZrO_2/TCPP	60
Fe_3O_4@ZrO_2/ZnTNBP	65
Fe_3O_4@ZrO_2/CoTNBP	73
Fe_3O_4@ZrO_2/ZnTCPP	95
Fe_3O_4@ZrO_2/CoTCPP	98

Photocatalysis process

It is generally believed that the photocatalytic activity of ZrO_2 is only in the range of UV light due to a broad Eg of about 5 ev.

So, being coated on the surface of Fe_3O_4 magnetic nanoparticles, with a low band gap of approximately 1.6 ev or lower can effectively absorb sunlight. The presence of porphyrin improved the photocatalytic performance of Fe_3O_4@ZrO_2 Magnetic nanoparticles.

As be seen in figure 8, under the visible light irradiation, photocatalytic process of Fe_3O_4@ZrO_2-Porphyrin was sensitived and with a photon transition, electron converted from the ground state to the excited state of porphyrin and turns to positive and negative charges. The generated electron not only transferred to the porphyrin surface but also injected into the conduction band of ZrO_2, owing to The CB level of ZrO_2 is near the CB of porphyrin. On the other hand, the electrons in the valence band (VB) of ZrO_2 are preferentially excited to its conduction band (CB) under irradiation and therefore generate an equal amount of

holes in its VB. The photogenerated holes transfer from the VB of ZrO_2 to the V_B of porphyrin. Therefore, the probability of electron–hole recombination can be reduced.

It is propability, Fe_3O_4 Superparamagnetic nanoparticles due to magnetic dipole interactions are used to separate the catalyst from suspension by an external magnetic field.

The accumulation of electrons in the CB of ZrO_2 can react with molecular oxygen to produce $^{\circ}O_2$. Similarly, the holes on the porphyrin surface can attract electrons from water and hydroxyl ions in porphyrin to generate $^{\circ}OH$ through an oxidative process. These produced radicals effectively destroying the methylene blue [17-19]. (Equation 1-6).

$$[Fe_3O_4@ZrO_2 - TNBP] + h\upsilon \rightarrow [Fe_3O_4@ZrO_2 - TNBP]^* \quad (1)$$

$$[Fe_3O_4@ZrO_2 - TNBP]^* \rightarrow Fe_3O_4@ZrO_2[TNBP]^+ + e^-_{CB} \quad (2)$$

$$e^-_{CB} + O_2 \rightarrow O_2^{\circ -} \quad (3)$$

$$h^+_{VB} + OH^- \rightarrow OH^{\circ} \quad (4)$$

$$O_2^{\circ -} + MB \rightarrow \text{Oxidation products} \quad (5)$$

$$OH^{\circ} + MB \rightarrow \text{Oxidation products} \quad (6)$$

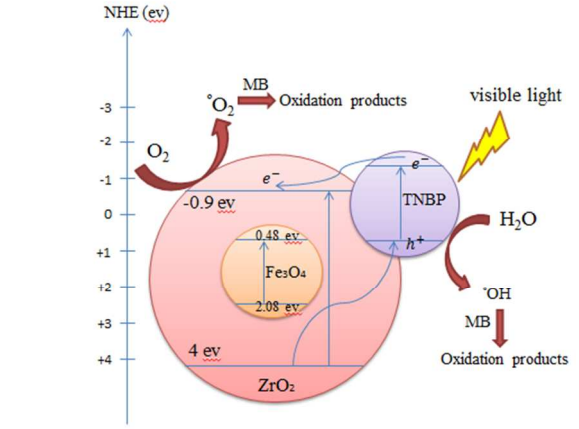

Fig 8. Schematic of photocatalytic mechanism.

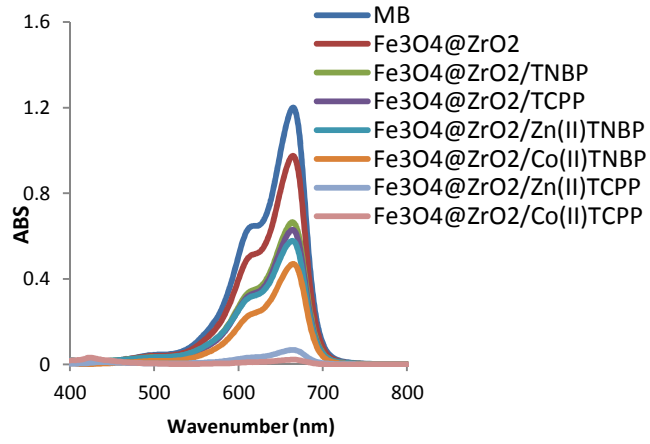

Fig 9. Absorption spectrum of distruction of MB(10 ml,10 ppm) after 3h irradiation by 10 mg catalyst in room temperature

Kinetic diagram

In order to obtain the degradation of Photocatalyst, synthetic graphs were drawn based on the reaction rate and obtained by the following equation:

$$D = [C_O - C/C_0] \times 100$$

C_o is the initial uptake of contaminants in the absence of photocatalysis and C is the adsorption after the exposure time. Samples taken in the first 30 minutes in the dark without light, and that the equilibrium adsorption - desorption is achieved. After it is completed in the presence of light, photocatalitic degradation done. As seen in the figure 10, the degradation of methylene blue in the absence of catalyst showed small amount in percentage. The nanoparticles of Zirconia iron oxide catalyst has a small amount of contaminant degradation. But there is a strong role for porphyrin in the photocatalytic degradation. CoTNBP and ZnTNBP deposition of nanoparticles on the substrate due to increased electron transfer reaction increases the efficiency degradation of photocatalyst. In this chart, the highest percentage of degradation is for catalyst particles sensitized with CoTCPP that due to its better stabilizion to the surface, can almost completely ruined methylene blue.

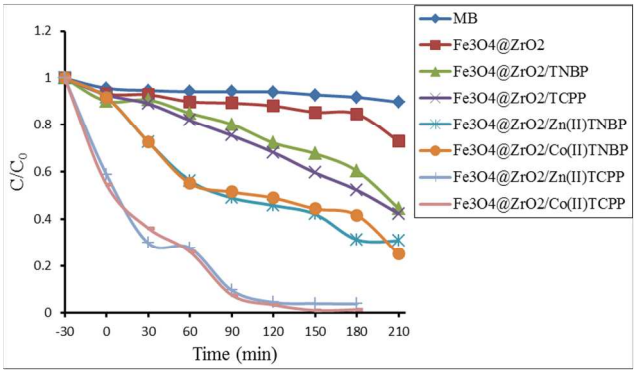

Fig 10. Kinetic diagram of MB (30 ml, 10 ppm) degradation under vs irradiation times by 30 mg catalyst

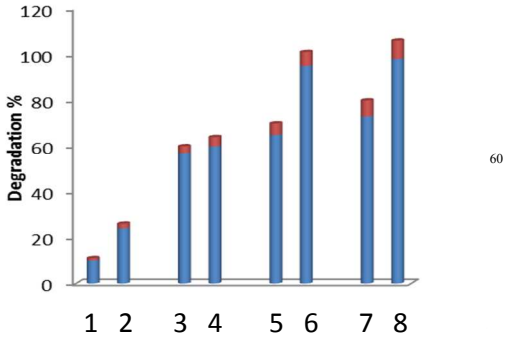

Fig 11. Degradation percentage of MB (10 ppm) using of 10 mg 1) Not Catalyst 2) $Fe_3O_4@ZrO_2$, 3) $Fe_3O_4@ZrO_2$/TNBP, 4) $Fe_3O_4@ZrO_2$/TCPP, 5) $Fe_3O_4@ZrO_2$/ZnTNBP, 6) $Fe_3O_4@ZrO_2$/ZnTCPP, 7) $Fe_3O_4@ZrO_2$/CoTNBP, 8) $Fe_3O_4@ZrO_2$/CoTCPP

Catalytic stability

After completing the degradation of Photocatalyst the catalyst was separated and washed several times with acetone and have not seen any change in its structure. FT-IR and DRS spectra of catalyst was confirmed the presence of porphyrin on the catalyst (Fig 12, 13).

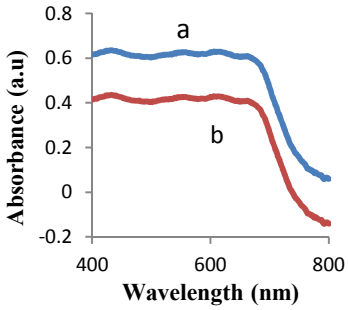

Fig 12. DRS spectra of Fe3O4@ZrO2/CoTNBP a) before completion the reaction b) after completion the reaction

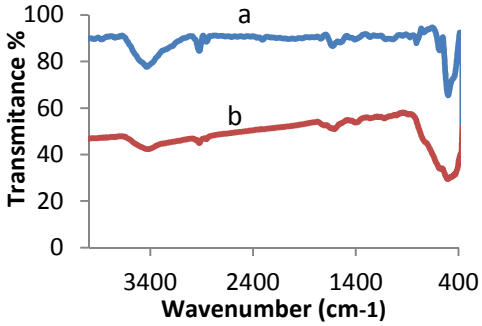

Fig 13. FT-IR spectra of of Fe3O4@ZrO2/ZnTNBP a) before completion the reaction b) after completion the reaction

Conclusions

The FT-IR, UV-Vis, DRS, SEM, XRD, ^{1}H-NMR and VSM techniques were used to characterize 5,10,15,20 tetrakis (4-naphtalen-2-yl-benzoate) porphyrin and its metal complexes with Zinc and Cobalt. These data approved the synthesis of this product and after that, to estimate the use of synthesized photocatalysis, degradation of methylene blue was done in the presence of light.

As a result, Metals in the center of tetra pyrrole rings of porphyrin increased more photocatalysis activity compared to the free porphyrin and increases the percentage degradation of methylene blue. Also, there is a strong role for porphyrin and metalloporphyrins in the photocatalytic degradation and deposition of nanoparticles on the substrate (increasing the electron transfer reaction will increased the efficiency degradation of photocatalyst).

Acknowledgments

The authors gratefully acknowledge the partial support from the Research Council of the Iran University of Science and Technology.

Notes and references

[a]*Department of Chemistry of Iran University of Science and Technology, Tehran, Iran. 16846_13114, Fax: 982177491204; Tel: 982177240516-7, E-mail: ghafuri@iust.ac.ir*

1 T. Tanaka, A. Osuka, *chemical society reviews,* 2015.
2 H. K. Hombrecher, S. Ohm and D. Koli, *Tetrahedron*,1996, **52**, 5441.
3 S. M. S. Ló, D. R. B. Ducatti, M. E. R. Duarte, S. M. W. Barreira, M. D. Noseda and A. G. Gonçalves,*Tetrahedron Letters*, 2011, **52**, 1441.
4 M. A. Schiavona, L. S. Iwamoto, A. G. Ferreirab, Y. Iamamotoa, M. V. B. Zanonic and M. D. Assisa, *J. Braz. Chem. So*, 2000,**11**, 458.
5 A. Faiz, V. Heitz and J. Sauvage, *chemical society reviews,* 2009,**38**, 422-442.
6 M. J. Crossley, P. J. Sintic, J. A. Hutchison and K. P. Ghiggino, *Organic and biomolecular chemistry,* 2005, **3**, 852.
7 M. J. Griffith, K. Sunahara, P. Wagner, K. Wagner, G. G. Wallace, D. L. Officer, A. Furube, R. Katoh, S. Mori and A. J. Mozer, *Chem. Commun*, 2012, **48**, 4145.
8 M. Niskanen, M. Kuisma, O. Cramariuc, V. Golovanov, T. I. Hukka, N. Tkachenkoa and T. T. Rantalab, *Phys.Chem. Chem. Phys*, 2013, **15**, 17408.
9 T. E. Shubina, H. Marbach, K. Flechtner, A. Kretschmann, N. Jux, F. Buchner, H. P. Steinru, T. Clark and J. M. Gottfried, *JACS,* 2007, **129**, 9476.
10 L. Sun, Y. Li, M. Sun, H. Wang, Sh. Xu, Ch, Zhang and Q. Yang**,***New J. Chem*, **2011**,*35*, 2697.
11 H. Jiang, P. Chen, Sh. Luo, X. Tu, Q. Cao, M. Shu, *Applied Surface Science*, 2013, **284**, 942.
12 Y. W. Wua,J. Zhanga, J. Liuc, L. Chena, Zh. Denga, M. Hana , X. Wei, A. Yu, H.Zhang, *Applied Surface Science*, 2012, **258**, 6772.
13 X, Huang, K. Nakanishi and N. Berova, *Chirality*, 2000, **12**, 237.
14 J. Rochford, E. Galoppini, *Langmuir,* 2008, **24**, 5366.
15 Zh. Xiangqing Li, Sh. Kang, L. Qin, G. Lib and J. Mu, *Chem. Commun*, 2014,**50**, 9064.
16 T. Nakazono, A. R. Parent, K. Sakai, *Chem. Commun***,** 2013, **49**, 6325.
17 G.Yao, J.Li, Y.Luo, W.Sun, *J. Mol.Catal* A, 2012, **361-362**, 2935.
18 CH.Wang, J.Li, G.Mele, G.M.Yang, F.X.Zhang, L.Palmisano, G.Vasapollo, *Applied Catalysis B*, 2007, **76**, 218226.
19 L. Gomathi Devi, R. Kavitha, *RSC Adv*, 2014, **4**, 28265.